

Nuclear Matter Spectral Functions by Transport Theory*

J. Lehr ^a, H. Lenske ^a, S. Leupold ^a and U. Mosel ^{a,b}

^a Institut für Theoretische Physik, Universität Giessen,
Heinrich-Buff-Ring 16, D-35392 Giessen, Germany

^b Institute for Nuclear Theory, University of Washington,
Box 351550, Seattle, WA 98195, USA
UGI-01-05

February 9, 2020

Abstract

Quantum transport theory is used to calculate the nucleon spectral function in infinite nuclear matter. A self-consistent description is obtained by utilizing the relations between collision rates and correlation functions. Static and dynamical self-energies are taken into account in the single particle propagators. The real parts of the non-static self-energy contributions are calculated by dispersion theory thus conserving the analyticity of momentum distributions. The transport theoretical spectral functions, momentum distributions, occupation probabilities and response functions are in close agreement with results of variational and other many-body theoretical calculations. The results indicate that the nucleon spectral functions are determined only by the average short-range correlation strength.

PACS numbers: 21.65.+f, 24.10.Cn

Keywords: nuclear matter, many-body theory, nucleon spectral function

*Work supported by BMBF, DFG and GSI Darmstadt

1 Introduction

A still controversial problem of nuclear many-body theory is the content of short-range correlations in nuclear matter and finite nuclei. The experimentally observed spectral functions, e.g. measured in $A(e, e'p)X$ [1] and more recent $A(e, e'pp)X$ [2] experiments clearly show the presence of a sizeable amount of high-momentum processes in nuclei not accounted for by mean-field dynamics. The observed pattern of the energy and momentum distributions indicates considerable admixtures of dynamical short-range correlations beyond the level of a static mean-field. While typical (e, e') experiments are performed on stable target nuclei corresponding to densities close to saturation extreme nucleon removal reactions with dripline nuclei like ^{11}Be and ^{19}C [3, 4] show increasing evidence for dynamical correlations also in low density nuclear matter.

An overall measure of short-range correlations in nuclear matter is the depletion of ground state momentum distributions from a pure Fermi gas picture by about 10%. The deviations are due to processes scattering nucleons from states inside the Fermi sphere into high momentum configurations which clearly are not of mean-field nature. As a result, the momentum distribution obtains a high momentum tail extending significantly beyond the Fermi surface. An important finding is that the magnitude and the shape of the high momentum component is almost independent of the system under consideration while the low momentum parts, especially in light nuclei, are affected by the shell structure and finite size effects. Hence, the high momentum tails of the spectral functions are likely to reflect a universal property of nuclear many-body dynamics at short distances.

The whole subject has become of renewed interest by the recent discussions on off-shell transport theory and in-medium cross sections [5], structure functions in a nuclear environment [6] and the QCD-related phenomenon of color transparency [7, 8]. The standard approach, taken for granted in most of the theoretical studies, is to assume that nucleons in a nuclear medium behave similar as in free space except for a change of the energy-momentum relation giving rise to a modified single particle spectrum but still concentrating the strength at the "on-shell" mean-field point. It has to be realized, however, that such a strict quasi-particle assumption is only partially supported by the available data. A general observation, e.g. in (e, ep) data is that the deviations increase for states deep inside the Fermi sphere.

Investigations on non-standard phenomena rely on a safe understanding of

the many-body theoretical aspects of short-range correlations. In fact, the results obtained from many-body theory describe the available data rather satisfactorily. The majority of the model calculations for infinite matter are using Brueckner and Dirac-Brueckner techniques, see e.g. [9, 10, 11, 12, 13, 14]. An explanation referring to the QCD aspects of strong interactions was proposed in [7]. In [15] a correlation dynamical treatment was applied. The Dirac-Brueckner calculations in [13], including hole-hole propagation, led to an extended and numerically rather involved energy-momentum structure of self-energies but the net effect on binding energies and occupation probabilities was surprisingly moderate. Most of the approaches use the quasi-particle approximation, i.e. assuming a sharp energy distribution for the nucleons in intermediate states (see e.g. [16]); only very recently self-consistent calculations, going beyond the quasiparticle approximation, have been performed [17]. Occupation probabilities in stable nuclei could be well described by second RPA [18] and by polarization self-energies [19], respectively, also in unstable nuclei [4, 3].

In this paper the quantum transport theoretical description of nucleon spectral functions in nuclear matter presented in [20] is discussed in more detail and extended in several aspects by considering additional observables. Since a long time transport theory is known to be *in principle* the correct description [21, 22, 23] for spectral functions. But explicit calculations on a realistic level were pending, also because an appropriate treatment of off-shell effects in transport equations was missing. The recent progress on implementing off-shell transport for heavy-ion and other nuclear collisions numerically [24, 25, 26] and theoretically [5] were important pre-requisites for the studies in [20] and the present work.

The theoretical background formulae are summarized in section 2. Since collision rates and correlation functions are directly related, the calculation of either of the two quantities depends on the knowledge of the other one. Theoretically, this rather involved self-consistency problem cannot be solved in closed form, but a practical approach is obtained by an iterative sequence of successive approximations for self-energies, spectral functions and collision integrals [13, 20].

Details of the numerical realization of the many-body theoretical relations are discussed in section 3. In extension of the previous work [20] here we include also dispersive self-energies into the single particle propagators. These non-static, i.e. energy and momentum dependent, self-energies are calculated by dispersion theory. In this way, the consistency of single particle dynamics

and spectral functions is enforced and, equally important, the analyticity of the results is guaranteed. The equations are solved using an average matrix element accounting primarily for the "hard" short-range collisions. Different to [20] here we include an energy and momentum dependent form factor. In section 3 results for nuclear matter spectral functions, ground state momentum distributions, occupation probabilities and response functions are presented. The agreement with results obtained with many-body theory by Benhar et al. [27] and Ciofi degli Atti et al. [28, 29] is striking. It confirms the universality of short-range correlations in nuclear systems and leads us to the conclusion that they are determined by an average matrix element representing globally the hard in-medium collisions.

2 Spectral Functions in Quantum Transport Theory

2.1 Transport Theoretical Relations

Here, the known fundamental relations of quantum transport theory [21, 22] for the description of non-stationary processes in an interacting quantum system are briefly summarized, following closely the presentation in [20]. In quantum transport theory the non-stationary processes which introduce a coupling between causal and anti-causal single particle propagation are described by the one-particle correlation functions

$$\begin{aligned} g^>(1, 1') &= -i\langle \Psi(1)\Psi^\dagger(1') \rangle \\ g^<(1, 1') &= i\langle \Psi^\dagger(1')\Psi(1) \rangle, \end{aligned} \quad (1)$$

where Ψ are the nucleon field operators in Heisenberg representation. Correspondingly, in an interacting quantum system the single particle self-energy operator includes correlation self-energies $\Sigma^{<>}$ which couple particle and hole degrees of freedom [21, 22]. Clearly, $g^{<>}$ and $\Sigma^{<>}$ are closely related. The wanted relation is obtained from transport theory. After a Fourier transformation to energy-momentum representation the self-energies are found as [21]

$$\begin{aligned} \Sigma^>(\omega, p) &= g \int \frac{d^3 p_2 d\omega_2}{(2\pi)^4} \frac{d^3 p_3 d\omega_3}{(2\pi)^4} \frac{d^3 p_4 d\omega_4}{(2\pi)^4} (2\pi)^4 \delta^4(p + p_2 - p_3 - p_4) \overline{|\mathcal{M}|^2} \\ &\times g^<(\omega_2, p_2) g^>(\omega_3, p_3) g^>(\omega_4, p_4), \end{aligned} \quad (2)$$

$$\begin{aligned}\Sigma^<(\omega, p) &= g \int \frac{d^3 p_2 d\omega_2}{(2\pi)^4} \frac{d^3 p_3 d\omega_3}{(2\pi)^4} \frac{d^3 p_4 d\omega_4}{(2\pi)^4} (2\pi)^4 \delta^4(p + p_2 - p_3 - p_4) \overline{|\mathcal{M}|^2} \\ &\times g^>(\omega_2, p_2) g^<(\omega_3, p_3) g^<(\omega_4, p_4).\end{aligned}\quad (3)$$

Here, $g = 4$ is the spin-isospin degeneracy factor and $\overline{|\mathcal{M}|^2}$ denotes the square of the in-medium nucleon-nucleon scattering amplitude, averaged over spin and isospin of the incoming nucleons and summed over spin and isospin of the outgoing nucleons.

Since both $g^{<>}$ and $\Sigma^{<>}$ describe the correlation dynamics, the spectral function can be obtained from either of the two quantities as the difference over the cut along the energy real axis. In terms of the correlation propagators, the spectral density is defined by

$$a(\omega, p) = i(g^>(\omega, p) - g^<(\omega, p)). \quad (4)$$

In a non-relativistic formulation the single particle spectral function is found explicitly as

$$a(\omega, p) = \frac{\Gamma(\omega, p)}{(\omega - \frac{p^2}{2m_N} - \text{Re}\Sigma(\omega, p))^2 + \frac{1}{4}\Gamma^2(\omega, p)}, \quad (5)$$

including the particle and hole nucleon self-energy Σ , which accounts for low-momentum, i.e. long-range, correlations as supported by the nuclear binding potential. The width of the spectral distribution is determined by the imaginary part of the self-energy,

$$\Gamma(\omega, p) = 2\text{Im}\Sigma(\omega, p) = i(\Sigma^>(\omega, p) - \Sigma^<(\omega, p)). \quad (6)$$

From Eqs. (2), (3) it is apparent that the high momentum, i.e. short range, components of nuclear interactions are of primary importance for the energy-momentum spreading of the single particle strength. For $\text{Im}\Sigma \rightarrow 0$, i.e. vanishing correlations, a sharp energy distribution given by a delta function is recovered, as assumed in the quasi-particle approximation.

The correlation propagators $g^{<>}$ are given by

$$g^<(\omega, p) = ia(\omega, p)f(\omega, p), \quad (7)$$

$$g^>(\omega, p) = -ia(\omega, p)(1 - f(\omega, p)) \quad (8)$$

in terms of the energy-momentum phase space distribution function $f(\omega, p)$. Since we are dealing with a system at $T = 0$, f reduces to

$$f(\omega, p) = \Theta(\omega_F - \omega) \quad (9)$$

with the Fermi energy ω_F . Therefore,

$$\Sigma^>(\omega, p) = 0, \quad \Gamma(\omega, p) = -i\Sigma^<(\omega, p) \quad \text{for } \omega \leq \omega_F \quad (10)$$

$$\Sigma^<(\omega, p) = 0, \quad \Gamma(\omega, p) = i\Sigma^>(\omega, p) \quad \text{for } \omega \geq \omega_F. \quad (11)$$

The energy and momentum dependent width Γ is obtained from the self-energies $\Sigma^>$ and $\Sigma^<$. Since these quantities themselves depend on Γ via the spectral function $a(\omega, p)$, the calculation has to be done iteratively.

The transport theoretical approach leads to single particle propagators including correlation self-energies to all orders by a complete resummation of the basic *sunset* diagram. The diagrammatic structure of Dyson equation defining the correlated propagators is shown in Fig. 1.

2.2 The Scattering Amplitude

Obviously, the correlation effects depend on the yet undetermined matrix element $\overline{\mathcal{M}}$. The question arises which processes contribute most significantly to $\overline{\mathcal{M}}$. Since the bulk of interactions giving rise to long-range mean-field interactions is already taken care of by the proper self-energies of particle and hole states the correlation functions and self-energies must both be determined by those parts of the fundamental interactions producing non-stationary effects beyond the mean-field. An estimate of the relevant interaction scales can be obtained by considering the physical situation, implying strong contributions from the high-momentum components of wave functions and interactions. From the observation that bulk self-energies include in their exchange parts momenta up to twice the Fermi momentum k_F a realistic estimate is to identify processes involving momentum transfers $q \gg 2k_F$ as the origin for short-range correlations. At the saturation point of nuclear matter with $k_F \sim 270$ MeV/c this corresponds to collisions with $q \gg 600$ MeV/c. Such processes are located in the interaction regime of the ω and ρ vector mesons, typically accounting for the short-range repulsion in nucleon-nucleon interactions. These processes are appropriately described by the short-range parts of a Brueckner G-matrix, accounting for the whole series of repeated meson-exchange processes.

In addition to the ladder-type interactions from the exchange of individual mesons also three-body (and possibly even higher order) interactions will contribute to short-range correlations in a nuclear medium. Such interactions involve the intermediate excitation of nucleon resonances which subsequently

decay back to the nucleon sector by an interaction with a third nucleon. Of similar importance are virtual excitations of NN pairs giving rise to the so-called Z graph contributions [30, 31]. The major contributions of these sub-nucleonic processes are known to be expressible to a good approximation in terms of an effective density dependent two-body interaction (see e.g. [32]), and, as such, will be part of $\overline{\mathcal{M}}$. The importance of such processes is indicated e.g. by the variational nuclear matter calculations of the Urbana group [32] showing a sizeable contribution from three-body interactions by subsequent pion exchange already at and below saturation density. Interestingly, Dirac-Brueckner calculations including the polarization of the nucleonic Dirac sea [30] and investigations of three-nucleon interactions [31] also point to the importance of dynamically generated repulsive short-range modes.

In this context it is of interest that the off-shell behavior of meson-exchange interactions is essentially determined by the mass of the exchanged boson. Hence, the matrix element $\overline{\mathcal{M}}$ will vary only weakly on off-shell momenta, at least on a scale of about $1\text{GeV}/c$, allowing to replace it to a good approximation by an energy and momentum independent constant, corresponding to an effective contact interaction. A similar approach is used in Landau-Migdal theory [33] describing interactions by the in-medium NN forward scattering amplitude at the Fermi surface. Different to conventional Landau-Migdal theory and to Ref. [20], here we will account for the remaining dependences at large momentum transfers by a global off-shell form factor $F(\omega, \vec{q})$, to be discussed below.

Taken together, these arguments lead to the expectation that $\overline{\mathcal{M}}$ is a quantity being almost independent of the specific system and the momentum transfer. The matrix element will reflect general properties of short-range nucleonic many-body dynamics, mediated by *hard* processes (on the scale of typical nuclear momenta) of universal character. Sensitivity to a single, specific channel seems to be unlikely considering the experience that short-range correlations are typically determined by a collection of interfering processes with strong mutual cancellations (see e.g. [31]). We assume universality and treat $\overline{\mathcal{M}}$ as a global parameter.

3 Numerical Approach and Results

3.1 Details of the Calculation

Diagrammatically, the particle- and hole-type transition rates $\Sigma^>$ and $\Sigma^<$, Eqs. (2) and (3), are of two-particle-one-hole (2p1h) and one-particle-two-hole (1p2h) structure, respectively, as shown in Fig. 1. In this respect, they are of the same basic structure as the polarization self-energies considered in many-body theoretical descriptions. However, while in many-body theory the polarization self-energies are typically included perturbatively in lowest order only by performing the integrations over intermediate 2p1h and 1p2h states with quasi-particle spectral functions, e.g. in Ref. [27] and also Refs. [18, 19], a more extended scheme accounting for higher order effects was presented in [20].

A previous attempt to extend the many-body scheme to higher order calculations was made in [13]. In order to keep the computational effort on a manageable level approximations on spectral functions of particle intermediate states had to be introduced. A new aspect of the transport theoretical approach of Ref. [20] was the fully self-consistent treatment of particle and hole strength functions. This is achieved by calculating the correlation self-energies with the self-consistently obtained spectral functions. This allows a non-perturbative summation of the whole series of $np\ mh$ intermediate states as shown in [20]. However, here we take advantage of the observation that already the first iteration agrees within a few percent with the final result of a fully iterated calculation. Because the main effect of higher order iterations is to redistribute a minor fraction of the strength into the high momentum tails of spectral functions the results presented here remain accurate on the energy-momentum scale relevant for the gross structures of spectral function and momentum distribution in pure nucleonic matter. Hence, these results also can be considered as re-confirming the validity of the perturbative treatment, assumed implicitly in previous investigations.

As already pointed out in [20] the numerical simplifications achieved when neglecting the off-shell dependence of \mathcal{M} are at the expense of violating analyticity, seen very clearly in an unrealistic behavior of the momentum distribution for $p \sim p_F$. These problems are corrected by introducing an energy and momentum dependent form factor

$$F(\omega_{\text{tot}}, \vec{p}_{\text{tot}}) = \frac{\Lambda^4}{\Lambda^4 + \left(\omega_{\text{tot}} + \frac{\vec{p}_{\text{tot}}^2}{4m_N}\right)^4} \quad (12)$$

that multiplies the average matrix element. Here $\omega_{\text{tot}} = \omega + \omega_2 = \omega_3 + \omega_4$, $\vec{p}_{\text{tot}} = \vec{p} + \vec{p}_2 = \vec{p}_3 + \vec{p}_4$ and $\Lambda = m_N$. Note that the form factor is symmetric under the exchange of the incoming and outgoing nucleon pair as seen from the delta function in Eqs. (2), (3). It is apparent that collisions at total energies and momenta beyond the scale of cut-off Λ will be suppressed by the form factor.

Theoretically, an even more important advantage of using a form factor is that the polarization contribution Σ_D to the real part of the single particle self-energies can now be calculated explicitly and consistently by means of a subtracted dispersion relation

$$\Sigma_D(\omega, p) = \left(\frac{p^2}{2m_N} - \omega \right) \mathcal{P} \int_{-\infty}^{\infty} \frac{d\omega'}{2\pi} \frac{\Gamma(\omega', p)}{(\omega - \omega') \left(\frac{p^2}{2m_N} - \omega' \right)} \quad (13)$$

where the on-shell point $\omega = \frac{p^2}{2m_N}$ is chosen as subtraction point. Note, that according to the above definition $\Sigma_D(\omega, p)$ is a real quantity.

In order to account for the static mean-field a density dependent but energy and momentum independent real self-energy Σ_0 is added, i.e. the real part of the self-energy becomes in total $\text{Re}\Sigma(q, \omega) = \Sigma_0 + \Sigma_D(q, \omega)$. In fact, the constant Σ_0 only serves to define the scale for the excitation energy ω which in our case is given by $\omega \geq \omega_F$. Since we are not interested in the dependence of our results on the density but only study the system at nuclear saturation density, we can absorb Σ_0 into ω , i.e. we re-define ω by $\omega + \Sigma_0$ for the following. Compared to [20], this corresponds to a shift of the energy scale by 52.6 MeV.

Starting from the vacuum spectral function of the nucleon

$$a_{\text{initial}}(\omega, p) = 2\pi\delta\left(\omega - \frac{p^2}{2m_N}\right), \quad (14)$$

one obtains from Eqs.(2), (3) the following simple expression for the self-

energies:

$$\begin{aligned}
\Sigma^<(\omega, p) = & \frac{\pm ig}{4\pi^3} \int_0^\infty dk \int_0^\infty dq \frac{kq^2 m_N}{p} \frac{1}{|\mathcal{M}_0|^2} F^2 \Theta(2m_N\omega + \frac{k^2}{2} - 2q^2 + p^2 + 2pk) \\
& \times \Theta(2pk - 2m_N\omega - \frac{k^2}{2} + 2q^2 - p^2) \\
& \times \Theta(\pm \frac{k^2}{2} \pm 2q^2 \mp 2m_N\omega \mp p_F^2) \Theta(\pm p_F^2 \mp \frac{k^2}{4} \mp q^2) \\
& \times \left(\Theta(\pm p_F - q \mp \frac{k}{2}) \pm \frac{p_F^2 - \frac{k^2}{4} - q^2}{kq} \Theta(q \pm \frac{k}{2} \mp p_F) \right).
\end{aligned} \tag{15}$$

Here $\vec{k} = \vec{p}_3 + \vec{p}_4$, $\vec{q} = (\vec{p}_3 - \vec{p}_4)/2$ and $p_F^2 = 2m_N\omega_F$. The upper sign refers to $\Sigma^<$, the lower one to $\Sigma^>$.

The average NN (off-shell) scattering amplitude \mathcal{M}_r , which determines the self-energies and spectral functions, was treated as a universal parameter. Adjusting it to the spectral functions from many-body calculations of Benhar et al. [27] we derive $\left(\frac{1}{|\mathcal{M}_0|^2}\right)^{1/2} = 207 \text{ MeV fm}^3$.

Relating the derived $\left(\frac{1}{|\mathcal{M}_0|^2}\right)^{1/2}$ to on-shell processes would correspond to a constant total NN cross section of about 20 mb accounting for roughly 2/3 of the commonly used value. The above strength, however, compares very well with the in-medium scattering amplitude of $+221.0 \text{ MeV fm}^3$ derived by Landau-Migdal theory from the nuclear equation of state for the Urbana interaction model [32], averaged over the Fermi sphere and spin and isospin. Since the calculations of [27] were performed in the correlated basis function approach, including also the three-body nucleon interactions in the Urbana prescription [32], we consider the derived value for $\left(\frac{1}{|\mathcal{M}_0|^2}\right)^{1/2}$ as a realistic overall measure for correlations in nuclear matter.

3.2 Nucleon Self-Energies and Spectral Functions

Before discussing the full spectral function Eq. (5), it is worthwhile to consider the influence of the form factor on the width and the spectral function without the dispersive Σ_D contribution. In Fig. 2 we show the results for the spectral nucleon width using i) the constant matrix element described above

and ii) the additional form factor from Eq. (12) for different momenta. It is worth noting that the influence of the form factor is completely different for energies below and above the Fermi energy: while for $\omega > \omega_F$ there is a strong suppression of the width for energies larger than 0.5 GeV, for $\omega < \omega_F$ the results for the calculations with and without form factor almost coincide. The reason for the weak influence for $\omega < \omega_F$ can be found in the step functions in Eq. (15). The nucleons are treated on-shell, thus Eq. (12) reduces to

$$F(k, q) = \frac{\Lambda^4}{\Lambda^4 + \left(\frac{k^2}{2m_N} + \frac{q^2}{m_N}\right)^4}.$$

Hence, for hole-type states where $k^2/2 + q^2 < 2p_F^2$ (see fourth step function in Eq. (15) for $\Sigma^<$), $F^2 > 0.999$ deviates only insignificantly from unity.

The observed behavior of the width in the calculations with and without form factor transmits to the spectral function, as can be seen in Fig. 3. The form factor strongly affects the high energy tails of the particle-type spectral functions at $\omega > \omega_F$ while for energies below ω_F the changes are negligible. This is a very satisfying result showing that the momentum distribution

$$n(p) = \int_{-\infty}^{\omega_F} \frac{d\omega}{2\pi} a(\omega, p) \quad (16)$$

is almost independent of the form factor.

We are now in the position to calculate the full spectral function, including also the dispersive self-energy Σ_D , Eq. (13). In Fig. 4 results for Σ_D and $\Gamma = 2\text{Im}\Sigma$ are displayed. Due to the decrease of Γ with increasing momentum also Σ_D is reduced. Therefore, the dispersive real part is expected to vanish at high p . This can be seen in Fig. 5, where the results for the spectral function with and without Σ_D are presented. At the on-shell point the difference of the two curves vanishes because $\Sigma_D(\frac{p^2}{2m_N}, p) \equiv 0$ by definition. Comparing to Fig. 3 the combined action of the form factor and Σ_D gives rise to a slight re-distribution of the strengths in the tail regions but leaves the region around the quasi-particle peak almost unaffected.

The influence of the analyticity of the self-energies on the momentum distribution (16) is illustrated in Fig. 6. Indeed, as anticipated before, the behavior of $n(p)$ below p_F is totally changed from a strong increase to a

smooth decrease towards p_F being now in agreement with many-body results e.g. [13, 27]. For momenta above p_F the differences between the two approaches are almost negligible.

3.3 Occupation Probabilities

Analyticity directly affects the normalization of the spectral function,

$$N(p) = \int_{-\infty}^{\infty} \frac{d\omega}{2\pi} a(\omega, p), \quad (17)$$

where conservation of probability requires $N(p) \equiv 1$. Whereas the calculation without Σ_D violates this condition - varying with momentum and reaching values of up to 30 % - the inclusion of the dispersive self-energy Σ_D leads to a properly normalized spectral function over the full momentum range.

The physical significance of Σ_D becomes evident by considering

$$Z(\omega, p) = \frac{1}{1 - \frac{\partial \Sigma_D(\omega, p)}{\partial \omega}} \quad (18)$$

which at the pole positions is known to describe the energy (and momentum) dependent wave function renormalization or spectroscopic factor accounting for the dissipation of single particle strength into the more complex many-body configurations. Results for $Z(\omega, p)$ at the on-shell energy $\omega = \frac{p^2}{2m}$ are displayed in Fig. 7. The overall shape follows roughly the spectroscopic factors from the many-body calculations of Benhar et al. [27], also shown in the figure for comparison. In magnitude our results are different, being higher by about 7% at the Fermi surface.

3.4 The Density Response of Nuclear Matter

Inclusive scattering of high-energetic electrons off nuclei measures directly the longitudinal and transversal density response functions from which information on the density-density correlation function is obtained [34]. Moreover, the nuclear response function is of current interest because it enters directly into investigations of scaling behavior and color transparency [6, 8]. At large momenta the density response is expected to be determined by universal properties of nuclear systems, being independent of the system under consideration.

Here, we neglect final state interactions (FSI) of the struck nucleon with the bulk and consider the density response of infinite nuclear matter in plane wave impulse approximation (PWIA) only. In the non-relativistic limit the density response (per energy) is defined by

$$S(\omega, p) = \frac{1}{V_F} \int \frac{d\varepsilon}{2\pi} \frac{d^3k}{(2\pi)^3} a(\varepsilon, k) \delta\left(\omega + \varepsilon - \frac{|\vec{p} + \vec{k}|^2}{2m_N}\right) \Theta(|\vec{p} + \vec{k}| - k_F), \quad (19)$$

where, according to our definition of spectral functions a normalization to the volume of the Fermi sphere,

$$V_F = \int \frac{d^3k}{(2\pi)^3} \Theta(k_F - k), \quad (20)$$

was introduced. The spectral function $a(\varepsilon, k)$ is seen to act in Eq. (19) as a source for the energy and momentum distribution of the ejected nucleons. At large momentum transfers where the FSI become negligibly small the PWIA results are expected to carry already the relevant information. In Fig. 8 the PWIA nuclear matter response function for several momenta are shown. In each case the maximum appears at the quasi-elastic (on-shell) energy $\omega_{QE} = \frac{p^2}{2m}$, as typical for quasi-free scattering. The width in each case correlates with the Fermi momentum. Results of calculations of Benhar et al. [27, 35] are also given in this figure as dashed lines. It is noticeable that in each case their response is shifted to higher energies compared to ours.

4 Summary and Conclusions

Correlations and nucleon spectral functions in nuclear matter were described by transport theory. Dispersive contributions to the nucleon self-energies are included, thus guaranteeing analyticity of spectral functions and momentum distributions. An important pre-requisite for this achievement was to include a form factor. The comparatively hard cut-off $\Lambda = m_N$ agrees with the assumed structure of the average matrix element $\overline{\mathcal{M}}$ as mainly given by processes involving momentum transfers well beyond twice the Fermi momentum of the system. The insensitivity of high momentum processes on bulk properties of a nuclear system and their weak off-shell dependence led us to describe dynamics by a momentum independent, universal matrix element, treated as the only adjustable parameter of the approach. Spectral functions

and momentum distributions for infinite nuclear matter at equilibrium were presented.

The good agreement with results from many-body calculations is impressive and confirms the approach. The energy and momentum dependencies of spectral functions and momentum distributions are well reproduced by our calculations, confirming also the conjectures of Danielewicz and Bertsch [23].

The results lead to the conclusion that the spectral functions and momentum distributions are dominated by phase space effects rather than by the off-shell momentum structure of interactions, at least in the momentum range up to 1 GeV.

The shape of the momentum distribution is obviously related to the magnitude of $\overline{\mathcal{M}}$: Increasing the value - corresponding to a stronger interaction amongst the nucleons - would increase the occupation of states above p_F and soften the Fermi edge. This close relationship constrains the admissible range of values. To the extent that higher order self-consistency is of minor importance, as indicated by our calculations, this also allows, in principle, to extract $\overline{\mathcal{M}}$ from spectral functions and the slopes of momentum distributions by precise measurements of the high momentum tails. However, we again emphasize that such a determination will only provide average information on short-range correlations in nuclei, not giving access to specific processes. Moreover, from the observed independence of $n(p)$ on form factor effects we expect that also the off-shell properties of interactions will play a minor role for momentum distributions, except for global properties as analyticity. This is easily understood if we accept that *hard* processes mediated by the (single or multiple) exchange of heavy mesons are the major source. Since the off-shell behavior of meson exchange interactions is essentially fixed by the mass of the meson it is clear that the off-shell momentum dependence of the underlying interactions will become important only on momentum scales well beyond 1 GeV.

References

[1] for a review see, e.g., P.K.A. de Witt Huberts, J. Phys. G (Nucl. Part. Phys.) **16** (1990) 507.

- [2] G. Rosner, in *Perspectives in Hadronic Physics* edited by S. Boffi, C. Ciofi degli Atti and M.M. Giannini (World Scientific, Singapore, 1998), p. 185.
- [3] H. Lenske, F. Hofmann, C.M. Keil, Rep. Prog. Nucl. Part. Phys. (in print).
- [4] D. Cortina-Lopez *et al.*, Euro. Phys. J. **A10** (2001) 49.
- [5] S. Leupold, Nucl. Phys. **A672** (2000) 475, nucl-th/0008036, Nucl. Phys. **A**, in print.
- [6] O. Benhar, V.R. Pandharipande, I. Sick, Phys. Lett. **B489** (2000) 131.
- [7] L. Frankfurt and M.I. Strikman, Phys. Rep. **76** (1981) 215.
- [8] O. Benhar, Phys. Rev. Lett. 83 (1999) 3130.
- [9] A. Ramos, A. Polls and W.H. Dickhoff, Nucl. Phys. **A503** (1990) 1; A. Ramos, A. Polls and W.H. Dickhoff, Phys. Rev. **C43** (1991) 2239.
- [10] S. Fantoni and V.R. Pandharipande, Nucl. Phys. **A427** (1984) 473.
- [11] H. Müther, G. Knehr and A. Polls, Phys. Rev. **C52** (1995) 2955.
- [12] F. de Jong and H. Lenske, Phys. Rev. **C54** (1996) 1488.
- [13] F. de Jong and H. Lenske, Phys. Rev. **C56** (1997) 154.
- [14] W.H. Dickhoff, Phys. Rev. **C58** (1998) 2807.
- [15] A. Peter, W. Cassing, J.M. Häuser and A. Pfitzner, Nucl. Phys. **A573** (1994) 93.
- [16] F. de Jong and R. Malfliet, Phys. Rev. **C44** (1991) 998.
- [17] W.H. Dickhoff, talk at the Workshop on Correlations in Nucleons and Nuclei, INT, University of Washington, March 2001.
- [18] H. Lenske and J. Wambach, Phys. Lett. **B249** (1990) 377.

- [19] F.J. Eckle, H. Lenske, G. Eckle, G. Graw, R. Hertenberger, H. Kader, F. Merz, H. Nann, P. Schiemenz and H.H. Wolter, Phys. Rev. **C39** (1989) 1662; F.J. Eckle, H. Lenske, G. Eckle, G. Graw, R. Hertenberger, H. Kader, H.J. Maier, F. Merz, H. Nann, P. Schiemenz and H.H. Wolter, Nucl. Phys. **A506** (1990) 159.
- [20] J. Lehr, M. Effenberger, H. Lenske, S. Leupold, U. Mosel, Phys. Lett. **B483** (2000) 324.
- [21] L.P. Kadanoff and G. Baym, Quantum Statistical Mechanics (Benjamin, New York, 1962).
- [22] W. Botermans and R. Malfliet, Phys. Rep. **198** (1990) 115.
- [23] G. Bertsch and P. Danielewicz, Phys. Lett. **B367** (1996) 55.
- [24] M. Effenberger and U. Mosel, Phys. Rev. **C60** (1999) 051901.
- [25] M. Effenberger, E.L. Bratkovskaya and U. Mosel, Phys. Rev. **C60** (1999) 044614.
- [26] W. Cassing and S. Juchem, Nucl. Phys. **A665** (2000) 377; Nucl. Phys. **A672** (2000) 417; Nucl. Phys. **A677** (2000) 445.
- [27] O. Benhar, A. Fabrocini and S. Fantoni, Nucl. Phys. **A505** (1989) 267; O. Benhar, A. Fabrocini and S. Fantoni, Nucl. Phys. **A550** (1992) 201.
- [28] C. Ciofi degli Atti, S. Simula, L.L. Frankfurt and M.I. Strikman, Phys. Rev. **C44** R7 (1991).
- [29] C. Ciofi degli Atti and S. Simula, Phys. Rev. **C53** 1689 (1996).
- [30] F. de Jong and H. Lenske, Phys. Rev. **C58** (1998) 890.
- [31] S.A. Coon, M.T. Peña, Phys. Rev. **C48** (1993) 2559; S.A. Coon, M.T. Peña, D.O. Riska, Phys. Rev. **C52** (1995) 2925.
- [32] A. Akmal, V.R. Pandharipande, D.G. Ravenhall, Phys. Rev. **C58** (1998) 1804.
- [33] A.B. Migdal, E.E. Saperstein, M.A. Troisky, D.N. Voskresensky, Phys. Rep. **192** (1990) 179.

- [34] W. Czyz, K. Gottfried, Ann. Phys. **45** (1963) 47.
- [35] O. Benhar, A. Fabrocini and S. Fantoni, Phys. Rev. Lett. **87** (2001), 052501.

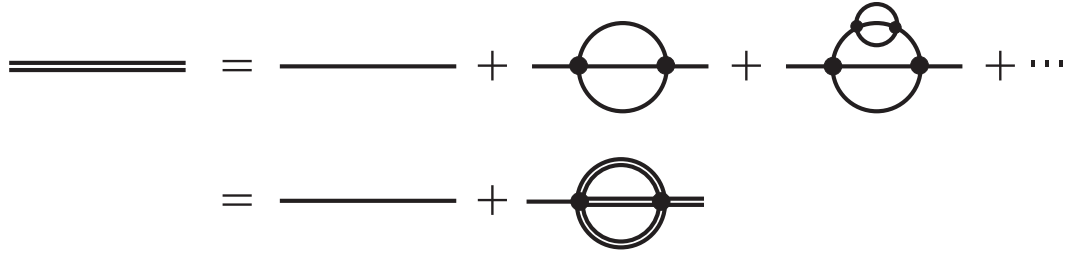


Figure 1: Diagrammatic structure of the self-consistent single particle propagator, indicated by a full line. The Dyson equation, corresponding to the complete resummation of the "sun-set" diagrams to all orders, is depicted in the second line.

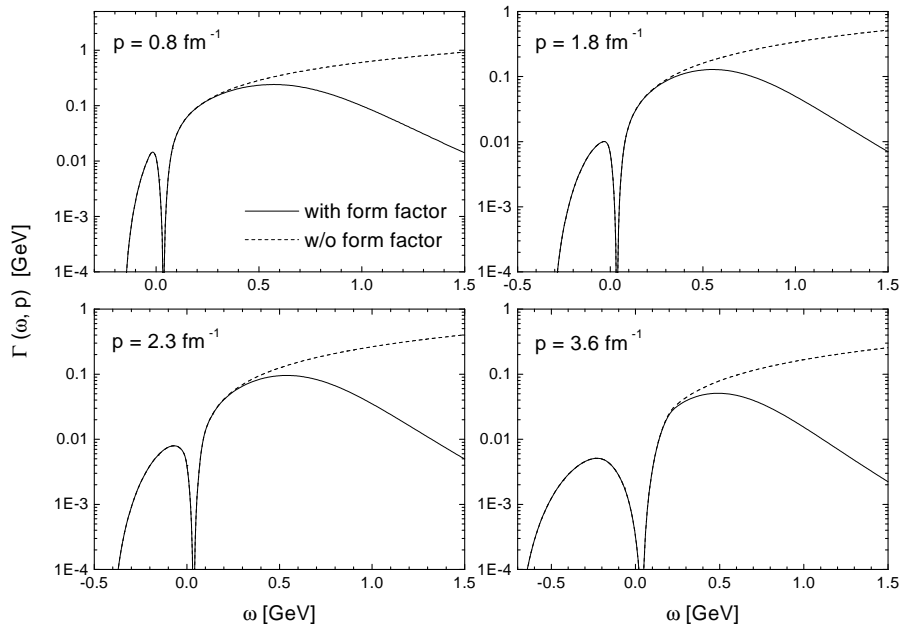


Figure 2: Widths of the nucleon spectral distributions for different momenta, calculated with (full) and without (dashed) form factor. Mainly the high-energy parts are affected by the off-shell form factor.

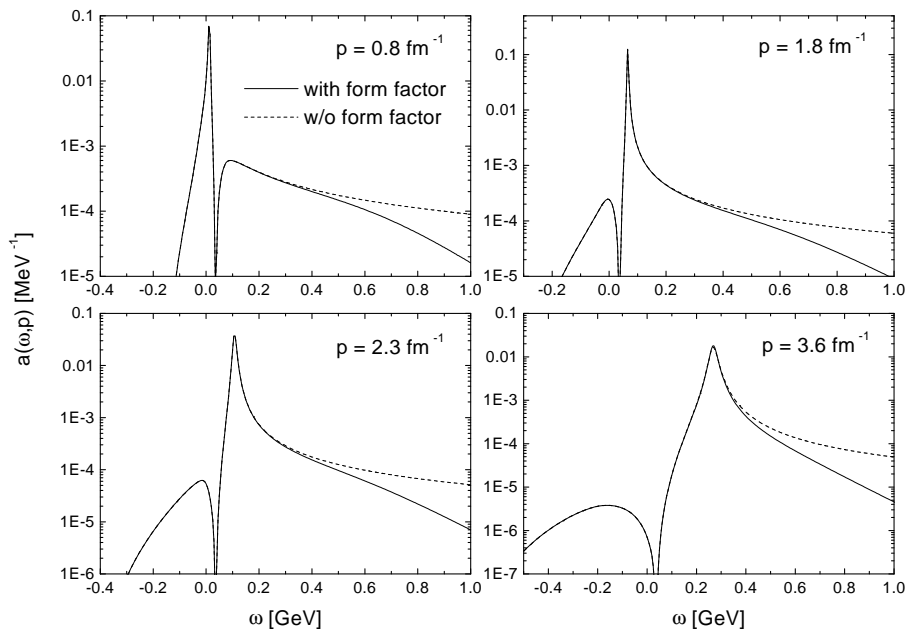


Figure 3: Influence of the form factor on the spectral function. Dispersive self-energies are not included.

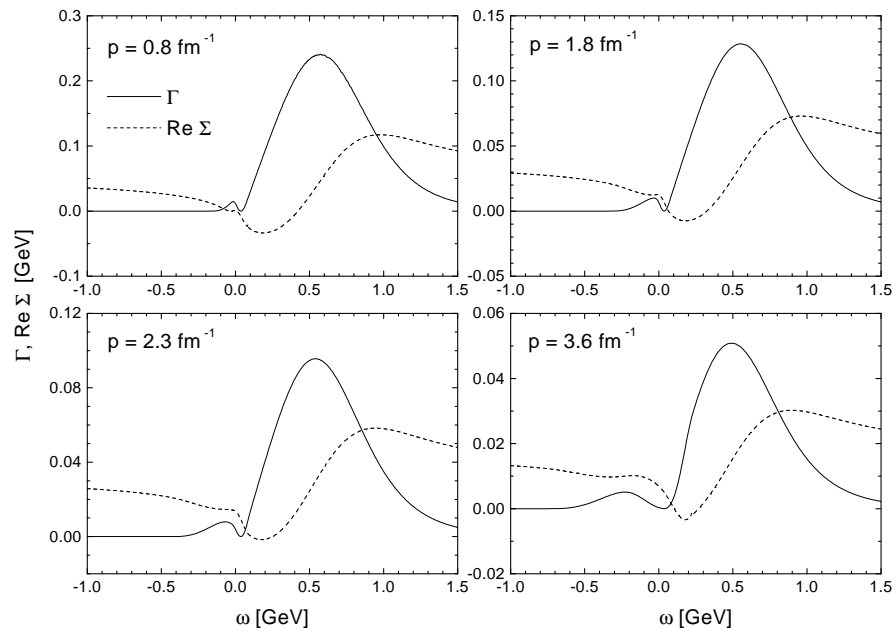


Figure 4: Width of the nucleon spectral function (full line) and real part of the dispersive self-energy (dotted line) for different momentum cuts.

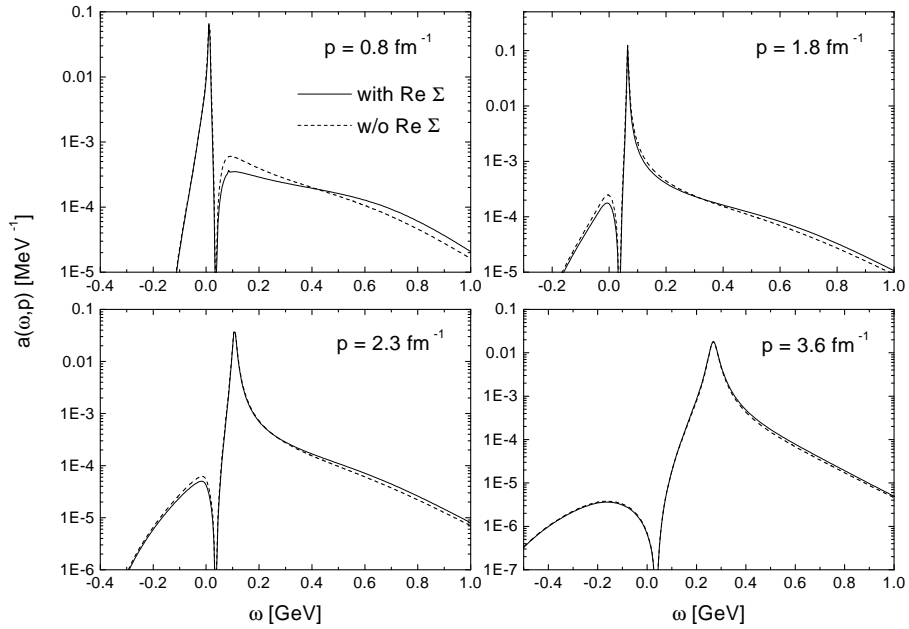


Figure 5: Nucleon spectral function at momenta below and above the Fermi momentum. Results with (full line) and without (dotted line) the real part of the dispersive self-energy are displayed. The quasi-particle peaks are clearly visible.

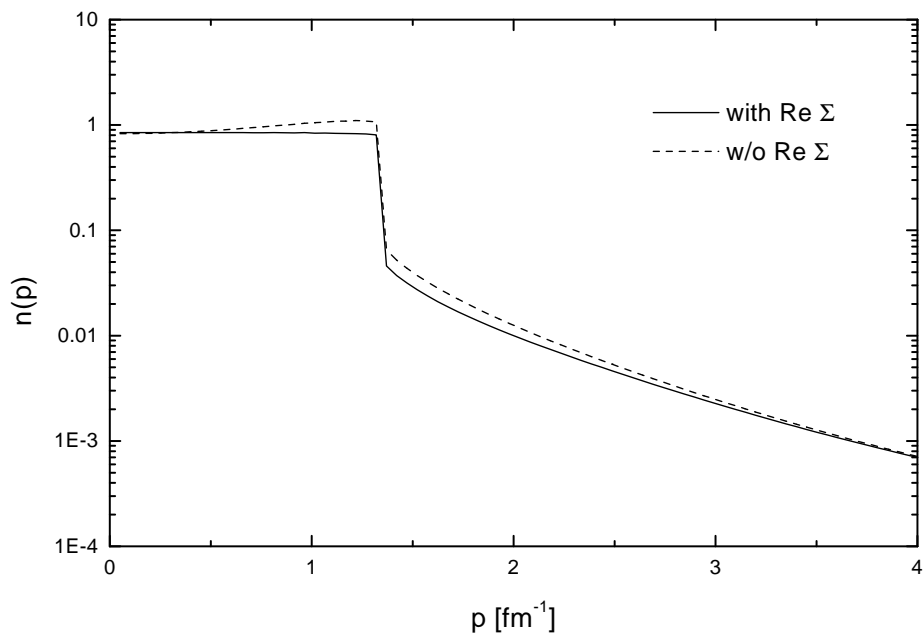


Figure 6: Nucleon momentum distribution in nuclear matter. Results neglecting analyticity (dashed) are also displayed.

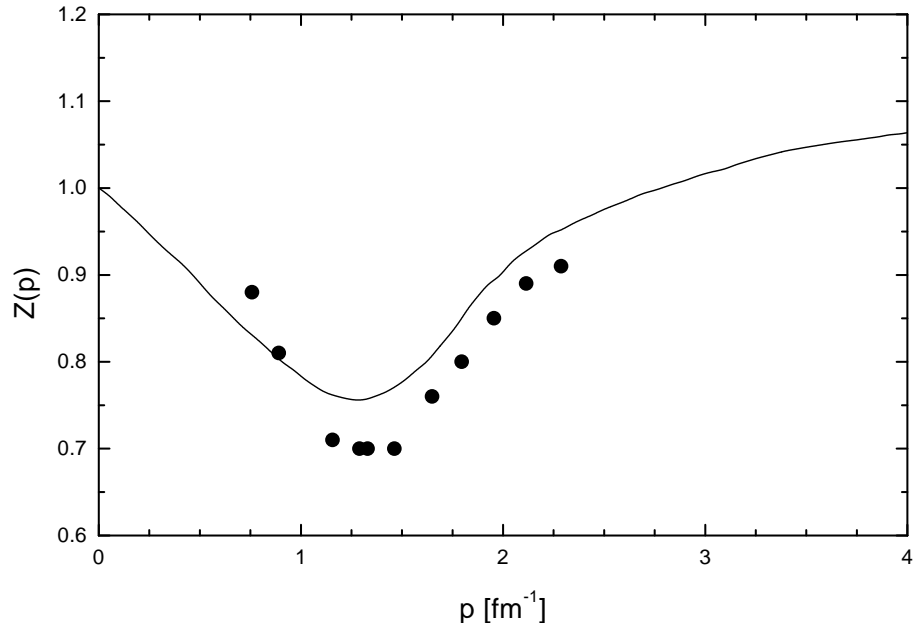


Figure 7: Nucleon spectroscopic factor in nuclear matter evaluated for the on-shell energy (see Eq. (18)). For comparison, results from the full many-body calculation of Benhar et al. [27] (dots) are also shown.

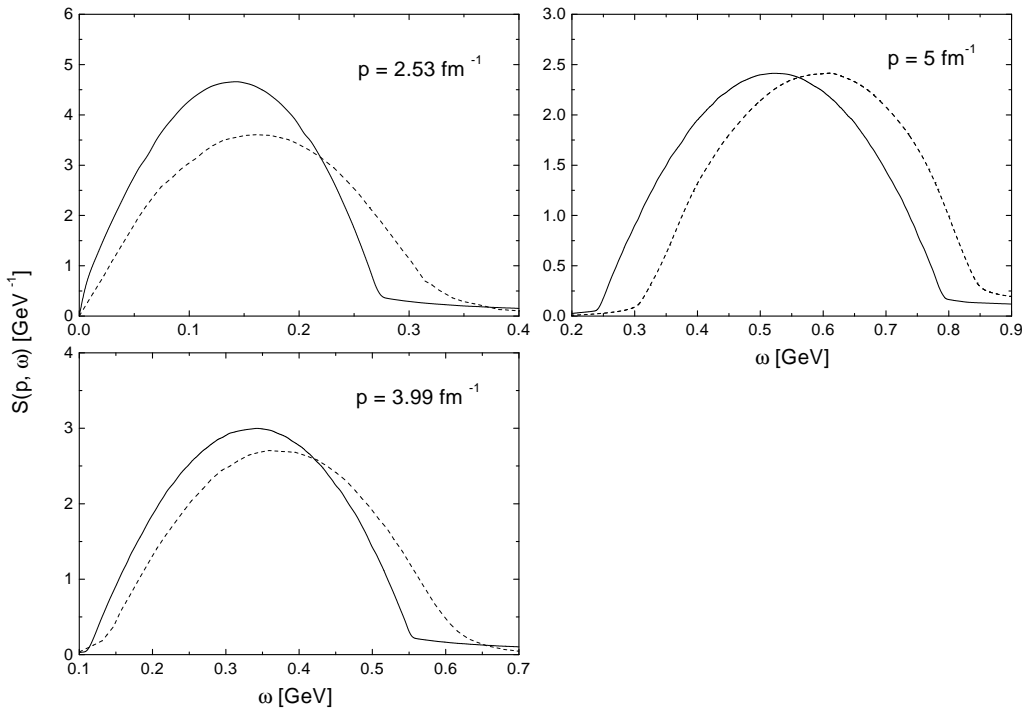


Figure 8: Nuclear matter density response functions, Eq. (19), at different momenta. The dashed lines show the results from [27, 35].